Journal of the Korean Physical Society, Vol. 51, No. 3, September 2007, pp. 967∼971

Study on the Low-Angle Surface Scattering of the Low-Energy Ions

K. S. Min, B. J. Park, J. B. Park, S. K. Kang and G. Y. Yeom*
Department of Advanced Materials Engineering, Sungkyunkwan University, Suwon 440-746

D. H. Lee
Memory Division, Samsung Electronics Co. Ltd, Yongin 449-711

(Received 13 November 2006)

The energy loss during the reflection of ions from a flat silicon surface at low incident angles and the scattering angles after the reflection were indirectly investigated for incident ion energies lower than 1 keV. Estimates of the energy loss during reflection from a flat silicon surface showed that increases in the incident ion energy and the angle increased the energy loss during the reflection from the reflector due to collisional energy loss. At an incident angle of 5°, the energy loss was about 12 % of the incident energy. After reflection, more than 99 % of the ions were neutralized, and the reflected atoms were scattered with a peak near a reflection angle of 10°, possibly indicating particle reflection by elastic collision.

PACS numbers: 12.14.M, 41.75.A
Keywords: Neutral beam etching, Nanoscale etch, Surface scattering

I. INTRODUCTION

As the semiconductor device sizes become smaller, electrical damage can be one of the most important issue because charged particles may cause serious damage to the device. As one of the methods to solve the problem, the generation of a neutral beam and the etching by a neutral beam are being studied [1–9]. By using neutral beam etching, the damage related to charging can be eliminated because no ions participate in the etching [10–12,17,18].

The neutral beams recently investigated for anisotropic etching are generated by low-angle charge exchange collision of an ion beam in the range from 1 to 500 eV with a flat surface. The characteristics of the neutral beam formed after the charge-exchange collision, such as the neutralization efficiency, the neutral beam energy and its distribution, the scattering angle of the neutral beam, *etc.*, are important in nanoscale device etching characteristics. When the ions are reflected from the surface, due to the overlap of the electron shell of the incident ions with the inner electron shell of the surface, the ions lose energy and are neutralized by the charge-exchange collision [13, 14]. The reaction phenomena between the surface and incident ions have been mostly studied for incident ion energies ranging from keV to MeV for ion implantation or surface analysis [15, 16]. However, incident energies less than 1 keV, which are important in the application of neutral beam etching, have not been investigated.

Therefore, in this study, the variations of the scattering angle and the energy loss after low-angle reflection of a low-energy (<1 keV) ion beam from a flat surface have been investigated using D_2 and SF_6 gases to understand the characteristics of the neutral beams used in neutral beam etching, which can be applied to various nanoscale etching procedures without charging damage.

II. EXPERIMENTS

Figure 1 shows the schematic diagram of the apparatus used to measure the energy loss and the scatter-

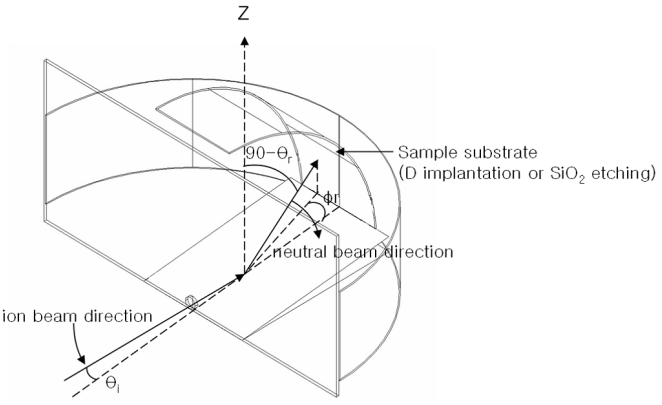

Fig. 1. Schematic diagram of the experimental system for the ion-beam reflection study.

*E-mail: gyyeom@skku.edu; Fax: +82-31-299-6565

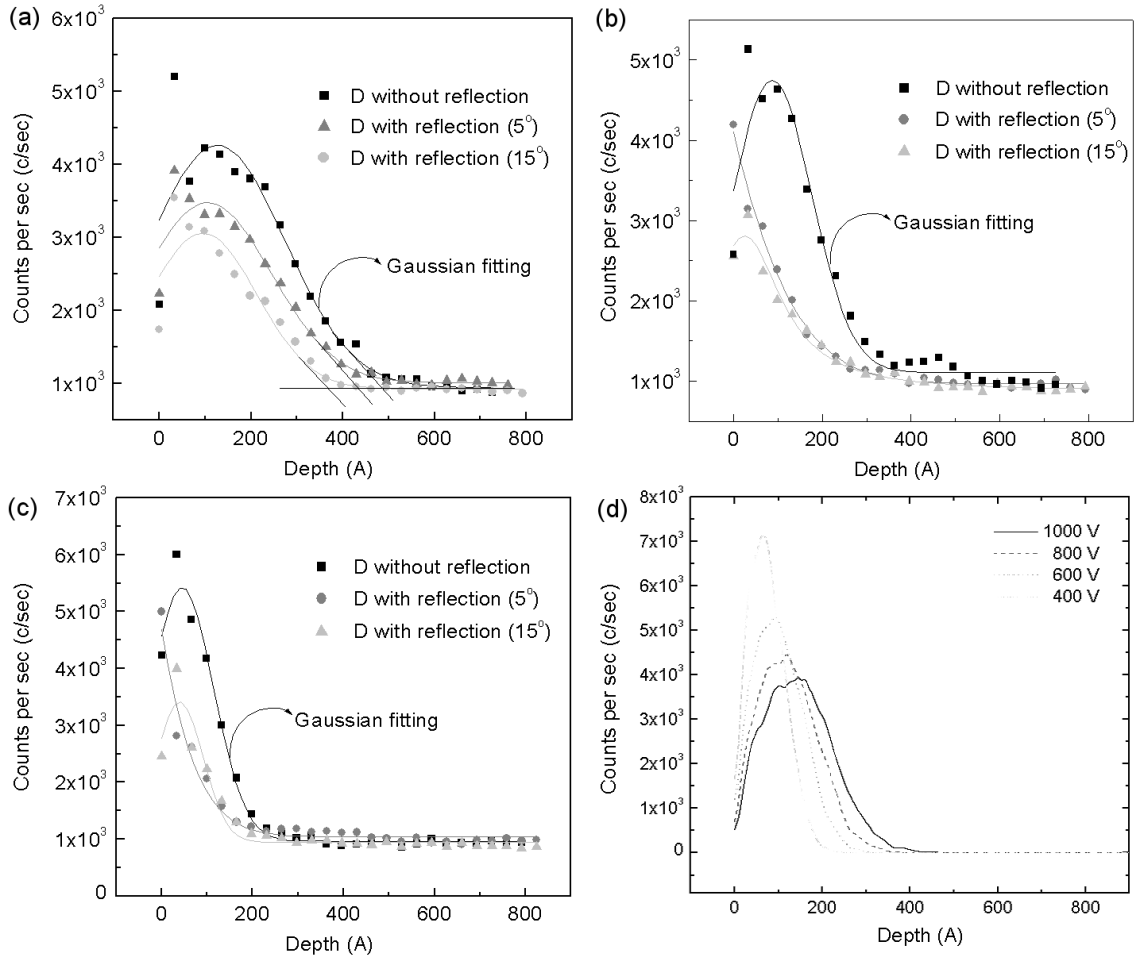

Fig. 2. SIMS depth profiles of deuterium ions or atoms on the silicon surface for various reflector angles for an incident ion energy of (a) 1 kV, (b) 600 V and (c) 400 V. (acceleration voltage: 400 V, 600 V and 1 kV; rf power: 300 W; D_2 gas flow rate 15 sccm; implantation time: 30 min). (d) is the simulation result of the D^+ implantation depth for various acceleration voltages.

ing angle after low-angle reflection of the ions from a flat surface. A 4-mm-diameter ion beam was formed by forming a 6-inch-diameter ion beam using a 6-inch-diameter inductively-coupled-plasma (ICP)-type ion gun with three grids operated by using a 13.56-MHz radio-frequency (rf) power, followed by passing the 6-inch-diameter ion beam through a 4-mm-diameter stainless-steel hole. The surface reflector was made of polished silicon and the incident angle θ, where $90° - \theta$ is the angle between ion beam's direction and silicon surface, was varied from 5 to 20°.

Using the ICP ion gun and the apparatus described above, we generated a 4-mm-diameter D^+ (deuterium) ion beam, which was reflected from a silicon reflector. The neutralization efficiency of the reflected D^+ ion beam was estimated using a Faraday cup by measuring the ion current before and after the reflection and was higher than 99 %. The (100) silicon samples with 30-Å SiO_2 were located at an angle normal to the deuterium beam, and the implantation depth was measured using a secondary ion mass spectrometer (SIMS, PHI 7200 TOF-SIMS). Using a TRIM code, we also estimated the D^+ ion implantation depth. 3000-Å-thick SiO_2 samples were located on a circular substrate holder at equal distances from the reflection point, as shown in Figure 1, and the SiO_2 samples were etched using a SF_x neutral beam generated with SF_6. The etch depths of SiO_2 measured at the different positions along the substrate holder of spherical-shell shape were used to estimate the scattering angle and the flux of the neutrals after the reflection at various angles.

III. RESULTS AND DISCUSSION

Figures 2(a)∼(c) show the deuterium depth profiles after irradiation with a deuterium ion beam and the neutral beam formed by the reflection at angles of 5 and 15° with energies of 400 V, 600 V and 1 kV, respectively. The rf power to the ICP gun and the D_2 gas flow rate were maintained at 300 W and 15 sccm, respec-

Table 1. Maximum implantation depth of the deuterium ions and atoms formed after the reflection of deuterium ions from the reflector measured for various acceleration voltages and reflection angles. The process conditions are the same as those in Figure 3.

Incidnet beam energy (V)	D^+ Implantation depth (A) (Simulation)	D^+ Implantation depth (A) (no reflection)	D^+ Implantation depth (A) (5° reflection)	D^+ Implantation depth (A) (15° reflection)
1000	430	486	433	368
600	310	321	294	276
400	240	233	212	186

tively. For comparison, the deuterium depth profiles in the silicon for the same conditions were estimated by using the TRIM code, and the results are shown in Figure 2(d). As Figure 2(d) shown, the deuterium depth profile showed a Maxwellian distribution, and the decrease in the deuterium incident energy of about 200 V decreased the penetration depth about 60 to 70 Å. The TRIM results shown in Figure 2(d) can be compared with the real deuterium depth profiles measured with SIMS for the same deuterium ion energies of 1 kV, 600 V and 400 V in Figures 2(a), (b) and (c), respectively. As figures shown, the deuterium penetration depth profiles could be fitted with a Gaussian fitting, and the maximum implantation depth was similar to the calculated maximum penetration depth even though there was about a 10 % difference for 1 kV.

However, as Figures 2(a)∼(c) shown, after the reflection from the reflector, the deuterium penetration depths decreased with increasing reflection angle, indicating energy loss during the reflection. A summary of the maximum deuterium depths of the deuterium ions into silicon and those after the reflection from low-angle reflectors is given in Table 1. From Figures 2(a)∼(c), a decrease in the penetrating deuterium flux can be also noticed with increasing reflection angle, possibly indicating an increase in random scattering with increasing reflection angle instead of total reflection.

From the simulation data and the experimental data for D^+ ion penetration into silicon in Figure 2 and Table 1, it can be seen that the decreases in the penetration depth with decreasing incident ion energy were similar to each other (that is, 60 ∼ 70 Å for the simulation data and 80 ∼ 90 Å for the experimental data with a decrease of 200 eV in the incident ion energy). Therefore, it can be calculated that a decrease of 10 Å in the penetration depth corresponds to a decrease of about 22.7 ∼ 24.2 eV in the incident energy. By comparing the maximum penetration depth of the deuterium ions without reflection and the deuterium atoms after reflection, as shown in Figure 2 and Table 1, the energy loss during the reflection can be indirectly calculated. Figure 3 shows the estimated energy loss after reflections at 5° and 15° for energies from 400 eV to 1 keV. As the figure shown, an increase in the incident ion energy from 400 V to 1 kV increases the energy loss from 47.7 to 128.3 eV for a 5° reflection (about 12 % of the incident ion energy) and from 84 to 285.6 eV for a 15° reflection (20 ∼ 30 %).

The loss of energy after the reflection can be explained from the ion-surface collision theory. When ions collide with the surface, the ions lose energy (ΔE_{bin}) due to hard-sphere collisions between the incident ions and surface atoms. In addition, the ions can loose energy by reactions with electrons on the surface, which is known as friction-like slowing or electron straggling, during the incoming and the outgoing paths before/after the hard collision [13,14]. If the energy losses during the incoming path and the outgoing path are represented as Q_1 and Q_3, respectively, the total loss of energy after the reflection (ΔE) can be written as

$$\Delta E = Q_1 + \Delta E_{bin} + Q_3. \tag{1}$$

In the case of Q_1 and Q_3, it can be shown that these can be written as the following equation [19]:

$$Q_1 = Q_3 = k\sqrt{E}, \tag{2}$$

where k is a parameter related to the screening length, and E is the particle energy. During the incoming path, the incoming ions are generally neutralized through resonant electron transfers with the surface or through the Auger process. In the case of hard collisions between the incident ions and the surface atoms, it is known that the energy loss, ΔE_{bin}, can be written as the following equation [13]:

$$\begin{aligned}\Delta E_{bin} &= \left(\frac{\gamma}{\gamma+1}\right) Q_{bin} \\ &+(E-Q_1)\left(\frac{2\cos\theta\sqrt{\gamma^2-\sin^2\theta}}{(1+\gamma)^2}\right) \\ &*\left\{1-\left[1-\left(\frac{\gamma(\gamma+1)}{\gamma^2-\sin^2\theta}\right)\frac{Q_{bin}}{(E-Q_1)}\right]^{1/2}\right\} \\ &= k[\gamma,\theta,Q_{bin},(E-Q_1)],\end{aligned} \tag{3}$$

Where $\gamma = M_2/M_1$ (mass ratio), θ is the incident angle, and Q_{bin} is the binary collision inelasticity. Therefore, the total loss of energy after the reflection (ΔE) increases with increasing incident ion energy and incident angle, similar to the results observed in Figure 3.

After the reflection from the reflector, the reflected atoms can be scattered at various angles. To understand

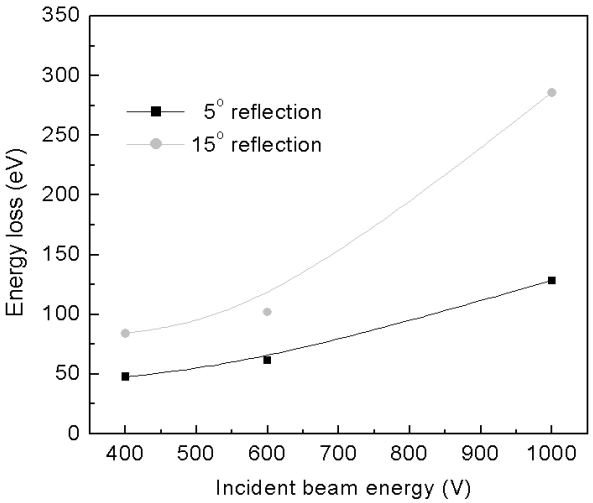

Fig. 3. Energy loss during reflection (neutralization) as a function of incident deuterium ion's energy from 400 V to 1 kV for incident angles of 5 and 15°.

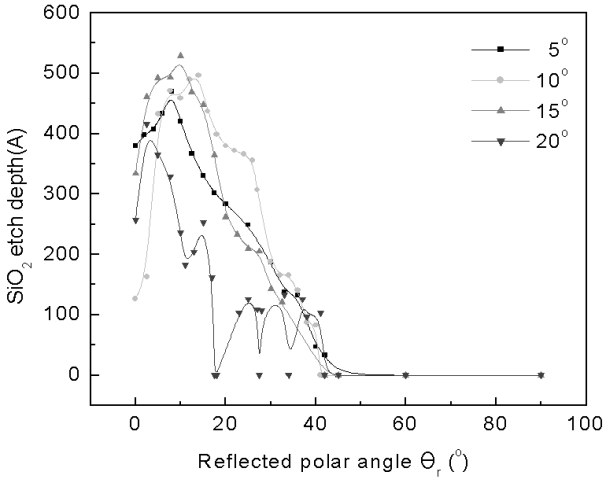

Fig. 4. SiO_2 etch depth distribution measured as a function of polar angle from the point of ion-beam reflection to measure the distribution of the reflected particles for incident angles from 5 to 20° (rf power: 400 W; SF_6 gas flow rate: 15 sccm; acceleration voltage: 400 V; etch time: 1 hour).

the scattering of the reflected atoms, we used SF_6 with 3000 Å thick SiO_2 samples located on the circular substrate holder as shown in Figure 1. Also, the SiO_2 samples were etched as a function of polar angle to measure the distribution of the reflected particles for various incident angles. The results are shown in Figure 4 for an rf power of 400 W, a grid acceleration voltage of 400 V and SF_6 flow rate of 15 sccm. As figure shown, at an incident angle of 5°, the SiO_2 etch depth was maximum near a polar angle of 10° and increasing the incident angle to 10° increased the reflected angle similar to the reflection of light on the mirror. However, a further increase of the incident angle not only decreased the maximum etch depth angle but also decreased the SiO_2 etch depth, possibly due to a decrease in the reflection of particles by elastic collisions.

IV. CONCLUSION

In summary, the loss of energy during the reflection of ions from a flat silicon surface at low incident angles and the scattering angles after the reflection were indirectly investigated for incident ion energies lower than 1 keV. The estimate of the energy loss during the reflection from a the flat silicon surface by measuring the differences in the deuterium atom depth profiles in silicon showed that increasing the incident ion energy and increasing the incident angle increased the energy loss during the reflection from the reflector by collisional energy loss. At an incident angle of 5°, the energy loss was about 12 % of the incident energy while at an incident angle of 15°, the energy loss was increased to 20 $\sim$ 30 %. After the reflection, more than 99 % of the ions were neutralized, and when the incident angle was increased from 5 to 10°, the maximum reflected angle estimated by the SiO_2 etching by using SF_6 increased from 10 to 15° while further increases in the incident angle decreased the maximum reflected angle, possibly due to the decreased possibility of particle reflection by elastic collision.

ACKNOWLEDGMENTS

This work was supported by the National Program for Tera-Level Nanodevices of the Korea Ministry of Science and Technology as a 21st Century Frontier Program

REFERENCES

[1] T. Yunogami, T. Mizutani, K. Suzuki and S. Nishimatsu, Jpn. J. Appl. Phys. **28**, 2172 (1989).
[2] A. Szabo and T. Engel: J. Vac. Sci. & Technol. A **12**, 648 (1994).
[3] M. J. Goeckner, T. K. Bennett, J. Y. Park, Z. Wang and S. A. Cohen, *Int. Sym. Plasma Process-Induced Damage* (Monterey, CA, AVS, 1997), p. 175.
[4] K. P. Giapis, T. A. Moore and T. K. Minton, J. Vac. Sci. & Technol. A **13**, 959 (1995).
[5] T. Yunogami, K. Yokogawa and T. Mizutani, J.Vac. Sci. & Technol. A **13**, 952 (1995).
[6] K. Yokogawa, T. Yunogami and T. Mizutani, Jpn. J. Appl. Phys. **35**, 1902 (1996).
[7] S. R. Leone, J. Appl. Phys. **34**, 2073 (1995).
[8] J. Yamamoto, T. Kawasaki, H. Sakaue, S. Shingubara and Y. Horiike, Thin Solid Films **225**, 124 (1993).
[9] H. Sakaue, K. Asami, T. Ichihara, S. Ishizuka, K. Kawamura and Y. Horiike, Mater. Res. Soc. Symp. Proc. **222**, 195 (1991).

[10] D. H. Lee, J. W. Bae, S. D. Park and G. Y. Yeom, Thin Solid Films **398**, 647 (2001).
[11] D. H. Lee, M. J. Chung, S. D. Park and G. Y. Yeom, Jpn. J. Appl. Phys. **41**, 1412 (2002).
[12] D. H. Lee, S. J. Jung, S. D. Park and G. Y. Yeom, Surf. Coat. Technol. **178**, 420 (2004).
[13] J. W. Rabalais, *Surface Chemical and Structural Analysis* (New Jersey, 2003).
[14] J. W. Rabalais, J. N. Chen, R. Kumar and M. narayana, J. Chem. Phys. **83**, 12 (1985).
[15] J. Lindhard and M. Scharff, Phys. Rev. **124**, 128 (1961).
[16] R. Schuch, H. Schone, P. D. Miller, H. F. Krause, P. F. Dittner, S. Datz and R. E. Olson, Phys. Rev. Lett. **60**, 925 (1988).
[17] D. H. Lee, B. J. Park, S. J. Kim, J. K. Lee, K. H. Baek, C. J. Kang and G. Y. Yeom, J. Korean Phys. Soc. **46**, 867 (2005).
[18] D. H. Lee, B. J. Park, K. S. Min and G. Y. Yeom, J. Korean Phys. Soc. **49**, 2307 (2006).
[19] O. Oen and M. Rohinson, Nuc. Inst. Meth. **132**, 647 (1976).